AUTOMATIC CLOUD AND CLOUD SHADOW DETECTION IN GF-1 WFV IMAGERY USING MULTIPLE FEATURES

Zhiwei Li[1], Huanfeng Shen[1], Huifang Li[1], Liangpei Zhang[2]*

[1] School of Resource and Environmental Sciences, Wuhan University, P. R. China
[2] State Key Laboratory of Information Engineering in Surveying, Mapping and Remote Sensing, Wuhan University, P. R. China

ABSTRACT

The cloud and cloud shadow are difficult to capture accurately in optical imagery because of insufficient spectral information. In this paper, an automatic multiple features combined (MFC) method is proposed for cloud and cloud shadow detection in GF-1 WFV imagery which includes three visible and one near-infrared bands. The local optimization strategy with guided filtering, and the proposed object-based filter combining geometry and texture features are used in the proposed method to refine cloud detection results and exclude non-cloud bright objects. The experimental results indicate that MFC performs well under different conditions.

Index Terms— cloud detection, cloud shadow, GF-1, object-based filtering, MFC

1. INTRODUCTION

As a kind of common contaminant in optical remote sensing data, cloud cover impedes optical satellite from obtaining clear views of the earth surface. Cloud and its shadow make negative influences on the use of imagery such as vegetation fraction estimation and land cover monitoring. Extracting the accurate distribution of clouds and cloud shadows in imagery to ignore or eliminate is an essential and important pre-processing step for precise application.

The wide field of view (WFV) imaging system onboard the Chinese GF-1 optical satellite has a 16-m resolution and four-day revisit cycle for large-scale Earth observation. Each WFV camera has four bands which are similar to Landsat ETM+ sensors in the first four bands spectral setting. The advantages of high temporal-spatial resolution and wide observation filed make GF-1 WFV imagery widely used in environment, agriculture, land resources, and emergency disasters etc. Cloud detection in GF-1 WFV imagery is a challenging work due to unfixed radiometric calibration parameters and insufficient spectral information.

In recent years, scholars have undertaken a great deal of research into cloud and cloud shadow detection for different types of remote sensing data such as AVHRR, MODIS and Landsat series imagery. ACCA [1], Fmask [2] and MSScvm [3] are typical algorithms designed for Landsat imagery which mainly rely on spectral features. Haze optimized transformation (HOT) which requires priori knowledge of the imagery is developed for the detection of haze/cloud and cloud shadow distributions in Landsat scenes [4, 5]. Methods based on machine learning include SVM and neural network are also applied in automatic cloud detection. Tmask [6] and MTCD [7] are multi-temporal methods used for cloud detection in multi-temporal imagery of the same area. Besides, cloud shadow detection is usually along with cloud detection [3, 8, 9]. Cloud shadow location in imagery can be predicted by geometrical calculations after cloud detection.

In this paper, an automatic multiple features combined method named MFC is proposed for cloud and cloud shadow detection in GF-1 WFV imagery. Experimental results suggest that our method works well in different ground cover condition, and it can also capture thin clouds around cloud boundary accurately merely relying on four optical bands.

2. THE MFC ALGORITHM

The input data for the MFC algorithm is TOA reflectance of all four bands in GF-1 WFV imagery. MFC first implements threshold segmentation and local optimization strategy with guided filtering based on spectral features to generate preliminary cloud mask. Then, an object-based cloud filter combining geometry and texture features is constructed to improve the cloud detection results and produce the final cloud mask. Finally, cloud shadow mask can be acquired by means of cloud and cloud shadow match and correction. Fig. 1 is the brief flow of MFC algorithm.

HOT index is used in MFC with the similar form as Fmask [2] to separate cloud from clear-sky pixels, it is

Fig. 1 Overall processing flow of MFC for automatic cloud/shadow detection.

an effective cloud extractor and widely used for cloud detection. Besides, thresholds for the visible bands relationship and single band reflectance are set to extract potential cloud. A rough cloud mask which includes relatively bright cloud is generated based on above spectral tests.

Local optimization strategy with guided filtering [10] is applied to refine the rough cloud mask and further capture thin cloud. The guided filter was used for cloud detection in RGB color aerial photographs [11]. It involves a guidance image I, an input image p, and an output image q which is supposed to a linear transform of I in a square window w_k at the pixel k:

$$q_i = a_k I_i + b_k \quad (\forall i \in w_k) \tag{1}$$

where i denotes a pixel coordinate in the square window w_k, and the two constant linear coefficients a_k and b_k in w_k can be defined by

$$a_k = \frac{\frac{1}{|w|}\sum_{i \in w_k} I_i p_i - \mu_k \overline{p_k}}{\delta_k^2 + \varepsilon} \tag{2}$$

$$b_k = \overline{p_k} - a_k \mu_k \tag{3}$$

where μ_k and δ_k^2 are the mean and variance of I in w_k, ε is the regularization parameter, $|w|$ is the number of pixels in w_k, and $\overline{p_k}$ is the mean of p in w_k. The final output value of the pixel i is defined by

$$q_i = \bar{a} I_i + \bar{b} \tag{4}$$

where $\bar{a}$ and $\bar{b}$ are the average coefficients of all windows overlapping pixel i.

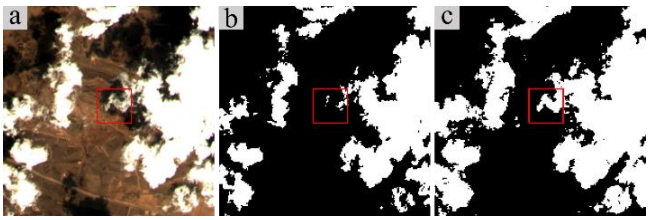

Fig. 2 Cloud mask refinement with guided filtering. (a) RGB composite guidance image. (b) Input binary cloud mask. (c) Output refined cloud mask after binary segmentation.

MFC uses guided filter as guided feathering in which a binary mask is refined to appear a gray alpha matte near the object boundaries. The preliminary cloud mask which involves thin clouds and more completed cloud boundaries is produced after segment the filtered output image to binary mask (Fig. 2).

In order to exclude bright non-cloud objects (such as snow, buildings, bright water body and coastlines) which cannot be effectively separated from cloud based on spectral features in preliminary cloud mask, an object-based cloud filter based on geometry and texture features is constructed. Cloud pixels in preliminary cloud mask connected in eight neighborhoods are merged to be an object. Fractal dimension (FD) of the object, which is derived form a spatial pattern analysis program named FRAGSTATS [12], and length width ratio (LWR) of object's rotating rounding rectangle are considered as two geometry descriptors which can be expressed as follow:

$$FD = \frac{2ln(girth/4)}{ln(area)} \tag{5}$$

$$LWR = \frac{max(length,width)}{min(length,width)} \tag{6}$$

where $girth$ and $area$ are for the object itself, $length$ and $width$ are for object's rotating rounding rectangle. FD indicates the complexity of object's shape which mirror the relationship between the girth and area. LWR is used for separate lathy non-cloud objects such as costlines and bright rivers from cloud.

Local binary pattern (LBP) texture descriptor in rotation invariant mode [13] is implemented to extract the texture features in the proposed object-based filter duo to its low computational cost and advantage of being illumination invariant. The LBP value in rotation invariant local binary pattern for the central pixel is computed according to

$$LBP_{P,R}^{ri} = min\left\{\sum_{p=0}^{P-1} s(x) \times 2^{[(p+l)modP]}\right\} \tag{7}$$

where $l \in [0, P]$, P is the number of involved neighbors, and R is the radius. The value of step function $s(x)$ equals 1 when the gray value of central pixel is greater than the sample point, and 0 if not. The histogram chi-square distance between the LBP histogram of the current object and trained template histogram can be the indicator which measures the texture similarity between the current object and clouds.

Owing to the object-based method to extract features, there will be no residual when a non-cloud object is determined to be removed from the cloud mask. Fig. 3 is examples in which bright water body and snow are excluded. MFC removes bright non-cloud objects from

cloud mask by comprehensive comparison of the geometry and texture features differences. The final cloud mask is then generated after post-processing steps include fill cloud holes and clear small objects.

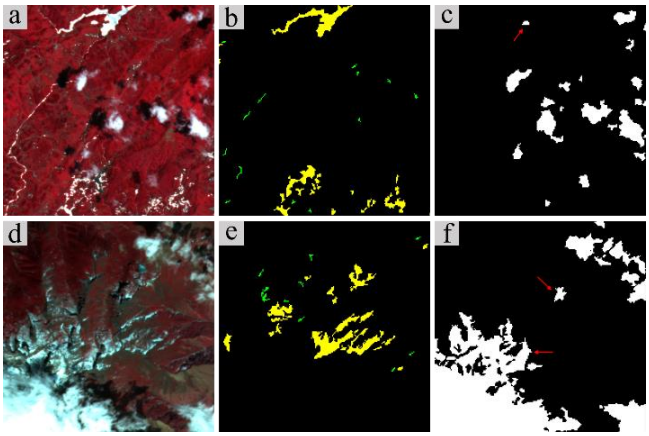

Fig. 3 Filtering non-cloud objects by using geometric and texture features. (a) False-color composite image. (b) Removed non-cloud bright objects (the green and yellow objects are excluded based on the geometric and texture features, respectively). (c) Cloud mask after filtering (objects marked with a red arrow denote non-cloud bright objects which are not excluded). (d)-(f) Another example of excluding snow from a cloud mask.

Cloud shadow location can be predicted by means of geometrical calculations after cloud detection. A morphological transformation called flood-fill [14] is applied to extract local potential shadow. Besides, considering that water body can be easily detected as shadow because of the minor differences in spectral characteristics, an object-based shadow filter based on geometry features is constructed to exclude water body from potential shadow mask after shadow extraction. Afterwards, shadow mask is generated.

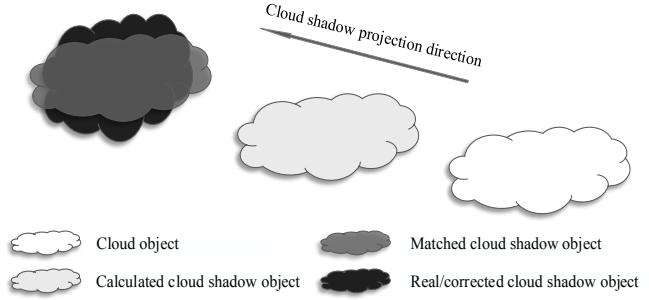

Fig. 4 Object-based cloud and shadow match and correction. (improved from Fmask by Zhu, 2012)

Object-based cloud and cloud shadow match [2] based on geometry similarity can be implemented after cloud mask and shadow mask are both acquired. Besides, MFC implements an object-based cloud shadow correction process (Fig. 4) in combination with the shadow mask to make sure that detected cloud shadow is completed as much as possible. Object-based cloud shadow correction is an extra step used for decreasing omission error of cloud shadow after cloud and cloud shadow match. In the proposed method, cloud shadow refinement with guided filtering and object-based cloud shadow filtering are also implemented to reduce cloud shadow matching errors and generate the final cloud shadow mask.

Finally, the morphological operation is necessary to improve the detection results. MFC sets higher priority for cloud than cloud shadow in the integrated mask. The final mask can be acquired after the aggregation of cloud mask and cloud shadow mask.

3. EXPERIMENTAL RESULTS

In our method, two modes are designed for different application purpose. Fast mode is used for rapidly estimating the cloud cover percentage, which can also generate a rough cloud and cloud shadow mask within 30 seconds for single WFV scene (about 17000×16000 pixels) on a laptop with Intel Core-i5 CPU, while precise mode usually costs 3~5 minutes to generate a more accurate mask. The main difference between the two modes is that fast mode downsamples the original scene to a smaller size during processing.

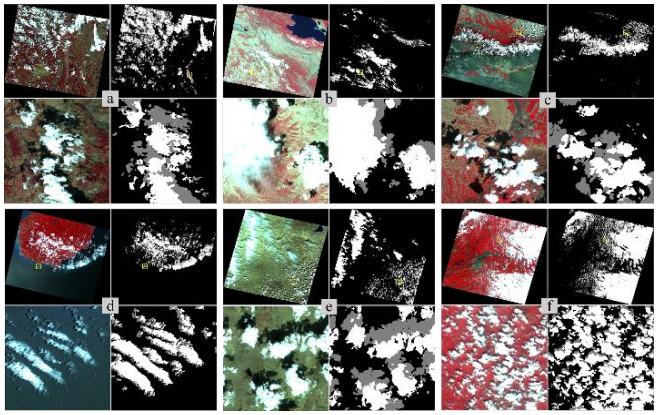

Fig. 5 Scenes and MFC masks used in accuracy evaluation.

The method was tested on 6 full scenes in different area in terms of fast cloud cover percentage estimation and precise cloud and cloud shadow detection. The reference cloud and cloud shadow masks are derived from manually drawing with Photoshop as previous study [1, 2] do. Cloud cover percentage derived from header file (with the official method), reference masks and fast MFC masks based on 6 scenes is used for error calculation of fast MFC. The mean absolute error of

MFC in fast cloud cover percentage estimation is 1.92% (5.10% in official method, 0.19% in precise MFC), and mean relative error is 0.112 (0.288 in official method, 0.013 in precise MFC). The accuracy evaluation results validate that MFC performs better than the official method in fast cloud cover percentage estimation.

Accuracy assessment for precise MFC measures the agreements and differences in precise MFC masks and the reference masks at the pixel scale. Precise MFC has achieved both average producer's and user's accuracy more than 90% for cloud and 70% for cloud shadow. The examples shown in Fig. 5 and accuracy evaluation results based on 6 scenes demonstrate the advantages of MFC in precise cloud and cloud shadow detection.

4. CONCLUSION

The MFC algorithm works well in automatic fast cloud cover percentage estimation and precise cloud and cloud shadow detection for WFV imagery. It can screen most of the thin clouds which usually cannot be easily detected. However, there still have some mistakes in cloud and cloud shadow mask generated by MFC owing to the shortcomings of algorithm itself and unavoidable radiometric calibration errors. Clouds in independent cloud area where are totally thin clouds may be missed in final mask. Besides, cloud shadows under low solar illumination condition or casted by thin clouds sometimes are not dark enough and hard to capture. Meanwhile, terrain shadow or dark water body connected with cloud shadows may be wrongly labeled as cloud shadow.

In the proposed method, local optimization strategy is implemented to capture thin clouds around cloud boundary, object-based filters combine geometry and texture features is proposed for excluding bright non-cloud objects from cloud mask, non-shadow objects from shadow and cloud shadow mask. In conclusion, the proposed method is effective and promising, it achieves good results with limited spectral bands. The general framework of cloud and cloud shadow detection proposed in this paper can be extended to more optical satellite imagery, including Chinese national CBERS and HJ series optical satellite imagery which has the similar spectral setting.

REFERENCES

[1] R. R. Irish, J. L. Barker, S. N. Goward, and T. Arvidson, "Characterization of the Landsat-7 ETM+ automated cloud-cover assessment (ACCA) algorithm," *Photogrammetric Engineering & Remote Sensing,* vol. 72, pp. 1179-1188, 2006.

[2] Z. Zhu and C. E. Woodcock, "Object-based cloud and cloud shadow detection in Landsat imagery," *Remote Sensing of Environment,* vol. 118, pp. 83-94, 2012.

[3] J. D. Braaten, W. B. Cohen and Z. Yang, "Automated cloud and cloud shadow identification in Landsat MSS imagery for temperate ecosystems," *Remote Sensing of Environment,* vol. 169, pp. 128-138, 2015.

[4] Y. Zhang, B. Guindon and J. Cihlar, "An image transform to characterize and compensate for spatial variations in thin cloud contamination of Landsat images," *Remote Sensing of Environment,* vol. 82, pp. 173-187, 2002.

[5] Y. Zhang, B. Guindon and X. Li, "A robust approach for object-based detection and radiometric characterization of cloud shadow using haze optimized transformation," *IEEE Transactions on Geoscience and Remote Sensing,* vol. 52, pp. 5540-5547, 2014.

[6] Z. Zhu and C. E. Woodcock, "Automated cloud, cloud shadow, and snow detection in multitemporal Landsat data: An algorithm designed specifically for monitoring land cover change," *Remote Sensing of Environment,* vol. 152, pp. 217-234, 2014.

[7] O. Hagolle, M. Huc, D. V. Pascual, and G. Dedieu, "A multi-temporal method for cloud detection, applied to FORMOSAT-2, VENμS, LANDSAT and SENTINEL-2 images," *Remote Sensing of Environment,* vol. 114, pp. 1747-1755, 2010.

[8] Y. Luo, A. Trishchenko and K. Khlopenkov, "Developing clear-sky, cloud and cloud shadow mask for producing clear-sky composites at 250-meter spatial resolution for the seven MODIS land bands over Canada and North America," *Remote Sensing of Environment,* vol. 112, pp. 4167-4185, 2008.

[9] N. R. Goodwin, L. J. Collett, R. J. Denham, N. Flood, and D. Tindall, "Cloud and cloud shadow screening across Queensland, Australia: An automated method for Landsat TM/ETM+ time series," *Remote Sensing of Environment,* vol. 134, pp. 50-65, 2013.

[10] K. He, J. Sun and X. Tang, "Guided image filtering," *IEEE Transactions on Pattern Analysis and Machine Intelligence,* vol. 35, pp. 1397-1409, 2013.

[11] Q. Zhang and C. Xiao, "Cloud detection of RGB color aerial photographs by progressive refinement scheme," *IEEE Transactions on Geoscience and Remote Sensing,* vol. 11, pp. 7264-7275, 2014.

[12] K. McGarigal and B. J. Marks, "FRAGSTATS: spatial pattern analysis program for quantifying landscape structure," 1995.

[13] T. Ojala, M. Pietikäinen and T. Mäenpää, "Multiresolution gray-scale and rotation invariant texture classification with local binary patterns," *IEEE Transactions on Pattern Analysis and Machine Intelligence,* vol. 24, pp. 971-987, 2002.

[14] P. Soille, *Morphological image analysis: principles and applications*: Springer Science & Business Media, 2013.